

# Conjugated polymers as molecular gates for light-controlled release of gold nanoparticles

*Maria Sanromán-Iglesias,<sup>†,‡</sup> Kai A. I. Zhang,<sup>§</sup> Andrey Chuvilin,<sup>‡,#</sup> Charles H. Lawrie,<sup>‡,#</sup> Marek Grzelczak,<sup>\*,†,#</sup> and Luis M. Liz-Marzán<sup>†,#</sup>*

<sup>†</sup>CIC biomaGUNE, Paseo de Miramón 182, 20009 Donostia-San Sebastián, Spain; <sup>‡</sup>Oncology area, Biodonostia Research Institute, Donostia-San Sebastián, Spain; <sup>§</sup>Max Planck Institute for Polymer Research, Ackermannweg 10, 55128 Mainz, Germany; <sup>‡</sup>CIC nanoGUNE Consolider, Av. de Tolosa 76, 20018 Donostia-San Sebastián, Spain; <sup>#</sup>Ikerbasque, Basque Foundation for Science, 48013 Bilbao, Spain

## AUTHOR INFORMATION

mgrzelczak@cicbiomagune.es (Marek Grzelczak)

**ABSTRACT**

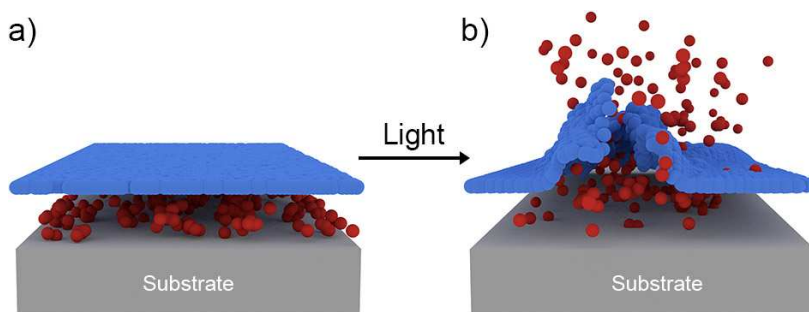
The remote release of nano-objects from a container is a promising approach to transduce chemical events into an optical signal. The major challenge in the development of such a system involves the use of a suitable molecular gate that retains aggregated particles and releases them upon applying an external stimulus. We show proof-of-concept experiments for the release of gold nanoparticles into an aqueous solution upon photodegradation of conjugated polymer thin films. Gold nanoparticles thus transduce light-induced chemical events into an amplified optical signal with a release rate of 2.5 nM per hour, which can be readily detected by the naked eye.

**KEYWORDS** Photodegradation, Remote release, Signal amplification, Reversible self-assembly, Gold nanoparticles

1  
2  
3 The release of cargo from a container is a core concept behind chemical signal amplification in  
4 living systems.<sup>1</sup> For instance, an individual hormone molecule interacting with a membrane  
5 receptor invokes multiple chemical processes in the cell interior, an efficient strategy to  
6 maximize redundancy in signaling and to eliminate error propagation. Similarly, signal  
7 amplification by the controlled release of nano-objects is a promising approach to mimic natural  
8 systems.<sup>2</sup> In this context, metal nanoparticles can transduce (bio)chemical events into an optical  
9 signal, thereby allowing (bio)sensing.<sup>3</sup> In a recent example, Grzybowski and co-workers reported  
10 the release of gold nanoparticles from micron-sized supercrystals by enzymatic digestion of a  
11 molecular shell acting as a gate.<sup>4</sup> Such nanoparticle-based signal amplification strategies are  
12 promising toward novel sensing strategies with simple practical implementation. The release of  
13 nanoparticles from a confined space is obviously a nontrivial task, requiring a judicious choice of  
14 chemical tools that make feasible the following steps: aggregation of nanoparticles, closing the  
15 molecular gate, and subsequently releasing the cargo. The major difficulty relies on the proper  
16 design of a molecular shell that is expected to retain the aggregated particles and release them  
17 only upon application of an external stimulus, such as light.  
18  
19  
20  
21  
22  
23  
24  
25  
26  
27  
28  
29  
30  
31  
32  
33  
34  
35  
36  
37

38 Owing to their outstanding optical properties, conjugated polymers are used in a number of  
39 light-related applications such as photovoltaics,<sup>5</sup> photodynamic therapy<sup>6</sup> or photocatalysis.<sup>7</sup>  
40 Although the polymers can be processed in liquid phase into a wide variety of functional forms  
41 (*e.g.* colloids, printable thin films), their degradation in the presence of light and/or oxygen is a  
42 drawback that requires novel synthetic approaches for improvement of their structural stability.<sup>8</sup>  
43 Interestingly, the structural instability of conjugated polymers can be seen as an advantage if the  
44 polymer is to be used as a photosensitive ‘gate’ to remotely release the nano-cargo into solution.  
45  
46  
47  
48  
49  
50  
51  
52  
53  
54  
55  
56  
57  
58  
59  
60

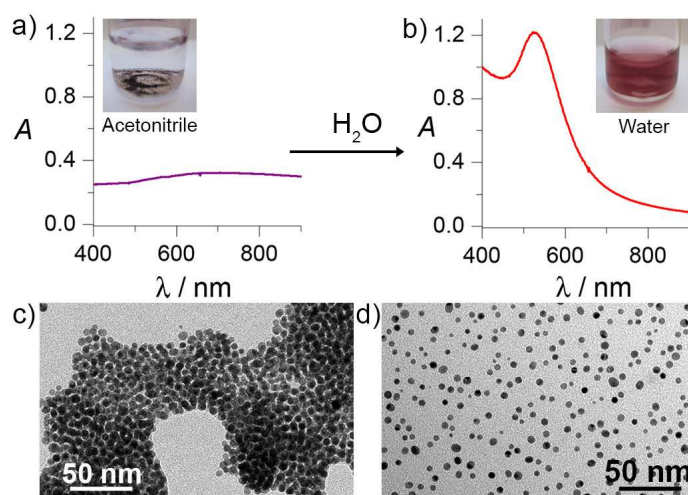
Our central hypothesis is described in Scheme 1: a conjugated polymer thin film covers gold nanoparticle aggregates, preventing their dispersion in water. Under light irradiation the thin film degrades, allowing nanoparticle release that is detectable by the naked eye. Therefore, the nanoparticles act as a signal transducer via amplification of structural and chemical changes in the polymer film.



**Scheme 1.** a) A thin polymer film (blue) prevents redispersion of gold nanoparticles (red) from a solid substrate (grey) into an aqueous solution. b) Visible light irradiation degrades the polymer releasing the nanoparticles into solution.

To evaluate our hypothesis, the nanoparticles acting as signal transducer need to remain aggregated in chloroform, (good solvent for the polymer) and get redispersed in water (bad solvent for polymer) with no need for stirring, shaking or sonication. We prepared reversible aggregates of gold nanoparticles by modification of a reported method,<sup>9</sup> in which the combination of two solutions of oppositely charged nanoparticles leads to the formation of aggregates at a specific pH. To ensure negative surface charge (-44.1 mV) at high pH, initially hydrophobic gold nanoparticles<sup>10</sup> ( $4.9 \pm 0.9$  nm) were functionalized with mercaptoundecanoic acid (MUA). On another batch, functionalization of the nanoparticles with 11-mercaptotetramethylammonium salt provided a positive surface charge of +18.1 mV (Figure S1).

1  
2  
3 In a typical aggregation process, the negatively charged nanoparticles (AuMUA) were mixed  
4 with positively charged nanoparticles (AuTMA) at pH 12, leading to phase separation, as  
5 reflected in a color change from reddish to violet. The aggregates were washed by centrifugation  
6 and resuspended in an aprotic polar solvent, such as acetonitrile (Figure 1a,c). Transfer of the  
7 aggregates into pure water led to immediate redispersion of the particles. Importantly, the  
8 nanoparticles in aggregated state can also be transferred onto a glass substrate and dried, but  
9 once immersed in pure water the nanoparticles diffuse into the solvent causing the coloration  
10 (Figure 1b,d). Such a spontaneous redispersion is crucial for our purpose, since the aggregates  
11 can be safely stored as a dry powder.



24  
25  
26  
27  
28  
29  
30  
31  
32  
33  
34  
35  
36  
37  
38  
39  
40  
41 **Figure 1.** Reversible aggregation of gold nanoparticles. UV-Vis spectrum (a) and TEM image  
42 (c) of aggregates formed by mixing oppositely charged nanoparticles, which remain aggregated  
43 in acetonitrile. UV-Vis spectrum (b) and TEM image (d) of nanoparticles redispersed in water.

44  
45  
46  
47  
48  
49  
50  
51 We used two different polymers, namely poly-Th-DPP<sup>11</sup> (Figure 2a – see SI for experimental  
52 details) and commercially available regiorandom-P3HT (Figure 2b). Both polymers formed thin  
53 films with a thickness of ~200 nm when spin-coated on the glass substrate (Figure 2e). UV-Vis  
54  
55  
56  
57  
58  
59  
60

1  
2  
3 spectroscopy provided valuable information on the optical features of the polymers, both in  
4 solution (chloroform), and as thin films (Figure 2c,d). In the case of poly-Th-DPP, the presence  
5 of two broad absorption bands at 380 and 614 nm suggested a high degree of conjugation  
6 between the donor and acceptor units within the rigid polymer chain. The intramolecular charge  
7 transfer between the thiophene and diketopyrrolopyrrole (DPP) segments originates the main  
8 absorption band at 614 nm (in solution), which shifted to 657 nm after spin-coating. The shift  
9 suggests an increased probability of low energy transitions due to long range ordering of  
10 aromatic molecules in the solid state,<sup>12</sup> facilitated by strong  $\pi$ - $\pi$  stacking interactions between the  
11 planar DPP skeletons of neighboring molecules.<sup>13</sup> We observed a similar optical behavior for the  
12 P3HT polymer, in which the maximum of the absorption band shifted from 428 nm in solution to  
13 441 nm after spin-coating, again due to an increased degree of order in the solid polymer.  
14  
15  
16  
17  
18  
19  
20  
21  
22  
23  
24  
25  
26  
27  
28  
29  
30  
31  
32  
33  
34  
35  
36  
37  
38  
39  
40  
41  
42  
43  
44  
45  
46  
47  
48  
49  
50  
51  
52  
53  
54  
55  
56  
57  
58  
59  
60

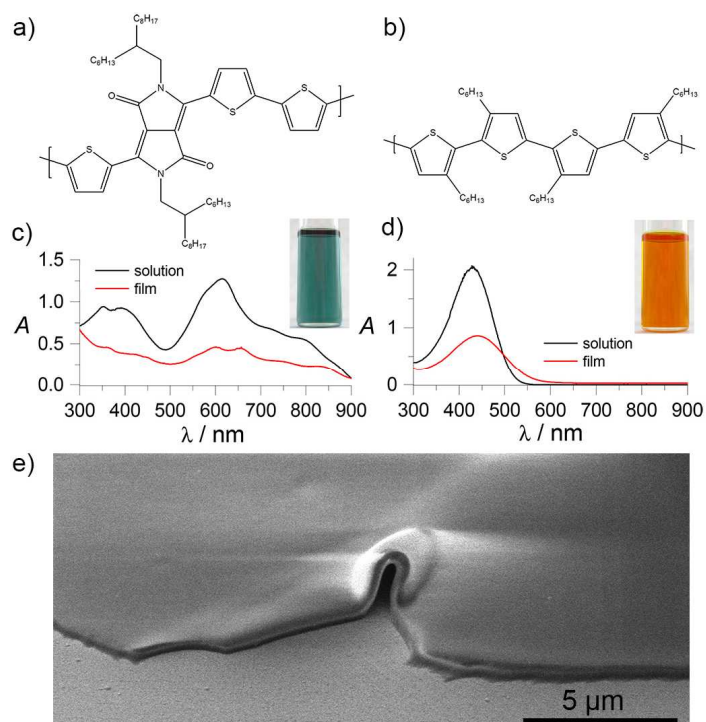


**Figure 2.** Chemical structure and UV-Vis spectra of (a, c) poly-Th-DPP and (b, d) P3HT polymers in chloroform solution (black lines) and as thin films on glass slides (red lines). (e) Representative SEM image of a poly-Th-DPP polymer film with a thickness of  $\sim 200$  nm.

To study film degradation we immersed the glass substrates ( $1 \text{ cm}^2$ ) covered with polymer films (P3HT or poly-Th-DPP) in quartz cuvettes filled with 1 mL of water and irradiated perpendicularly with white light ( $350 - 1100 \text{ nm}$ ,  $150 \text{ mW/cm}^2$ ) for 2 hours at  $40^\circ \text{C}$ . Exposure of the substrate to light led to a gradual decay of the optical absorption, whereas no changes were observed if stored in the dark. The effect of irradiation could be readily observed by eye, indicating physical changes in the film (Figure 3).

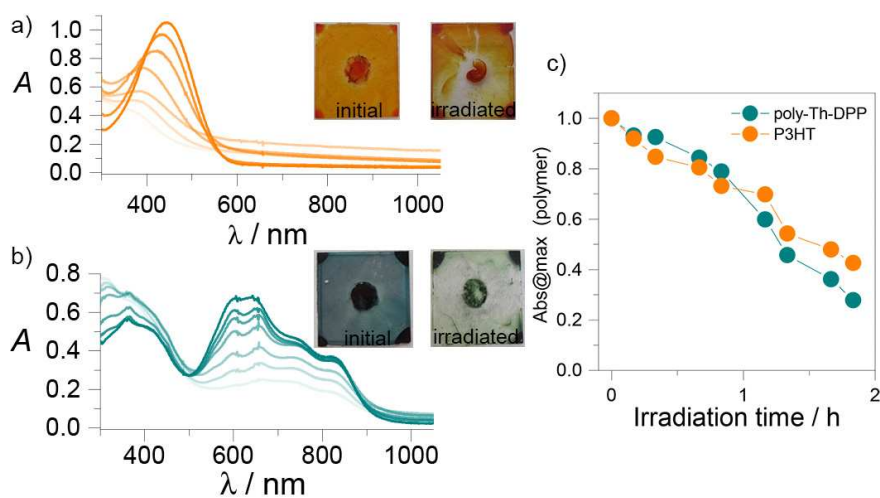


**Figure 3.** Photodegradation of polymer films. (a,b) Time-dependent UV-Vis monitoring of P3HT (a) and poly-Th-DPP (b) films under irradiation with visible light. Inset: photographs of the films before and after irradiation. (c) Variation of maximum absorbance with irradiation time, showing a similar degradation rate for both polymers.

1  
2  
3 For P3HT, the absorption maximum at 440 nm showed a linear decay accompanied by a  
4 blueshift of ~65 nm (Figure 3a),<sup>14</sup> which originated from the reduction of the  $\pi$ -conjugation  
5 length caused by the breakage of double bonds in the thiophene units.<sup>15</sup> Detailed MALDI-TOF-  
6 MS characterization of P3HT films before and after irradiation confirmed the fragmentation of  
7 the polymer into smaller subunits (Figure S2), as recently reported.<sup>16</sup> In the case of poly-Th-  
8 DPP, the irradiation led to absorption damping at longer wavelengths (> 500 nm), without  
9 blueshift (Figure 3b). We postulate that the DPP units are more susceptible to the attack by  
10 reactive oxygen species than thiophene units, which could lead to the opening of double 5-  
11 member rings. Progressive degradation of DPP units prevents intramolecular charge transfer  
12 from thiophene to DPP, which explains damping of the band without noticeable blueshift. This  
13 hypothesis was confirmed by MALDI-TOF MS analysis, which showed absence of polymer  
14 fragmentation after irradiation (Figure S3). This behavior was expected since DPP-based  
15 materials exhibit excellent chemical stability.<sup>17</sup> Raman scattering spectroscopy further confirmed  
16 the degradation of the polymer films (Figure S4). For P3HT, the characteristic peaks (721 and  
17 1454  $\text{cm}^{-1}$ ) disappeared completely while the Raman spectrum of the poly-Th-DPP film  
18 remained unchanged after irradiation.

19  
20  
21  
22  
23  
24  
25  
26  
27  
28  
29  
30  
31  
32  
33  
34  
35  
36  
37  
38  
39  
40  
41 We used the spin-coating technique to cover the aggregates with polymer films and found that  
42 mechanical pressing of the relatively large aggregates (>1  $\mu\text{m}$ ) was crucial, prior to spin coating,  
43 to avoid the leakage of the nanoparticle into the solution beneath the polymer thin film of ~200  
44 nm (see Figure S5 for SEM analysis of the partially covered aggregates). On the other hand, if  
45 the polymer was drop-casted from a chloroform onto the aggregates, thicker films were formed  
46 that prevented nanoparticle release, even under prolonged irradiation (Figure S6).  
47  
48  
49  
50  
51  
52  
53  
54  
55  
56  
57  
58  
59  
60



1  
2  
3 Irradiation of the polymer film on the aggregates led to the remote release of nanoparticles into  
4 water, as observed by the naked eye (Figure 4a inset). Time-dependent monitoring of the  
5 solution showed a gradual increase of a localized surface plasmon resonance band, in agreement  
6 with an increased Au nanoparticle concentration in solution (see Figure 4a for poly-Th-DD and  
7 Figure S7 for P3HT). We estimated the release rate of the nanoparticles by recording the  
8 absorbance at 400 nm, which can be translated into the number of the particles per unit volume.<sup>18</sup>  
9  
10 The faster release rates of 2.6 nM per hour for poly-Th-DPP, as compared to 0.75 nM per hour  
11 for P3HT (Figure 4b), was rather surprising especially considering that the degradation rate is  
12 similar for both polymers (Figure 3c). This is likely due to a higher absorption of the light  
13 emitted from the halogen lamp<sup>a</sup> by the green-colored poly-Th-DPP, as compared to P3HT. We  
14 exclude the possibility of a thermal effect caused by plasmon heating since poly-Th-DPP absorbs  
15 efficiently in the visible, thereby inhibiting absorption by the aggregated nanoparticles.  
16  
17 Additionally, the plasmon-heating effect would involve power densities of incoming light in the  
18 order of W per cm<sup>2</sup>. We used white light with a power density of ~150 mW/cm<sup>2</sup>, which is too  
19 low to induce plasmon heating. Relatively strong light absorption by the polymer and the lack of  
20 chemical changes in the poly-Th-DPP film suggests mechanical deformation of the film.  
21  
22 Although the local temperature during irradiation is hard to estimate, it is suggested that a local  
23 phase transition can facilitate mechanical changes in the film. Careful inspection of the films by  
24 SEM analysis showed that the initially smooth films (Figure 4c and S8) became porous, with  
25 multiple cracks and hollow spaces (Figures 4d and S9), facilitating the release of the particles.  
26  
27 On the other hand, photodegradation of P3HT is dominated by chemical processes – as observed  
28 by UV-Vis, Raman, MALDI -, which lead to formation of intermediate radicals that can affect  
29 the stability of the nanoparticles and hinder their release. SEM analysis revealed the presence of  
30  
31  
32  
33  
34  
35  
36  
37  
38  
39  
40  
41  
42  
43  
44  
45  
46  
47  
48  
49  
50  
51  
52  
53  
54  
55  
56  
57  
58  
59  
60

remaining particles beneath the irradiated P3HT film, which was not the case for Poly-Th-DPP (for comparison see Figure S9 c and f).

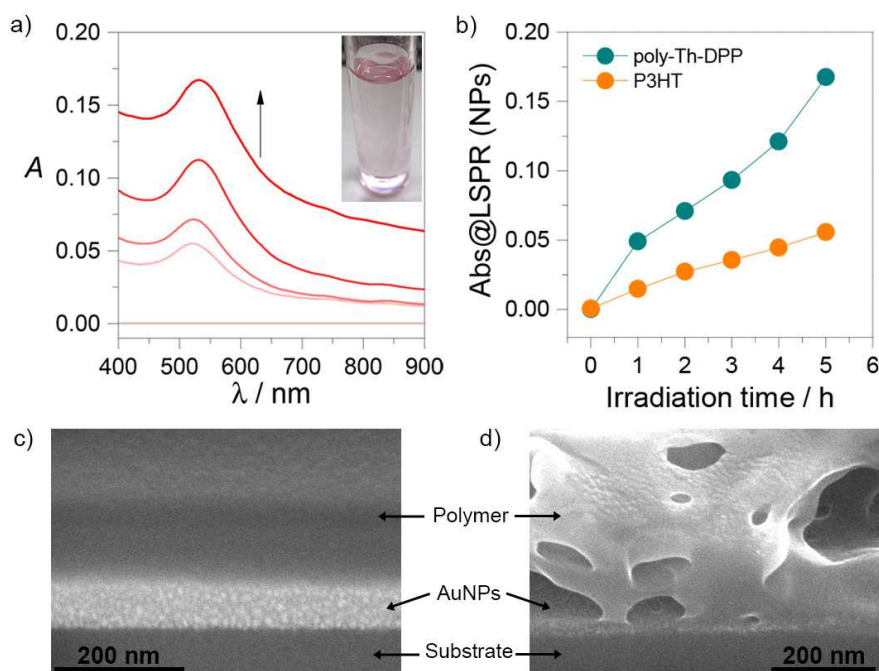


**Figure 4.** Nanoparticle release under irradiation. (a) Time-dependent UV-Vis spectra of the solution with gradually increasing concentration of nanoparticles. Inset: photograph of the solution containing released particles. (b) Time-dependent absorbance changes of the gold nanoparticle solution during irradiation, showing faster release for the poly-Th-DPP film. (c,d) SEM images of the P3HT film (cross-section) before (c) and after (d) irradiation.

In summary, we demonstrated proof-of-concept experiments for the remote release of nanoparticles into aqueous solution by photodegradation of a thin polymer film that acted as a molecular gate. We concluded that the release of nanoparticles was faster when using a polymer that absorbs a wider spectral range matching the features of the incident light. Although the observed release rate is still slow, there is room for improvement by optimization of parameters such as film thickness, particle size or irradiation intensity. However, since the particles release

1  
2  
3 can be readily monitored by eye, we expect that our approach will open up new possibilities in  
4  
5 the field of sensing. For example, functionalization of the polymer with receptor molecules could  
6  
7 hinder (or boost) molecular gate opening in the presence of light, which could lead to the  
8  
9 emergence of an optical signal induced by a recognition process at the molecular level.  
10  
11  
12  
13

#### 14 ASSOCIATED CONTENT

15  
16  
17 Supporting Information. Experimental details, UV-Vis spectra, Raman and SEM analysis of the  
18  
19 initial nanoparticles and films. This material is available free of charge via the Internet at  
20  
21 <http://pubs.acs.org>.  
22  
23  
24  
25

#### 26 AUTHOR INFORMATION

27  
28  
29 \*Email: [mgrzelczak@cicbiomagune.es](mailto:mgrzelczak@cicbiomagune.es)  
30  
31  
32  
33

#### 34 Notes

35  
36  
37 <sup>a)</sup> For the spectral profile of the lamp used in all experiments see Figure S7.  
38  
39

40 The authors declare no competing financial interests.  
41  
42

#### 43 ACKNOWLEDGMENT

44  
45  
46 This work was supported by the Spanish Ministerio de Economía y Competitividad  
47  
48 (MAT2013-46101-R) and the Instituto de Salud Carlos III (Proyectos integrados de excelencia  
49  
50 ref: PIE13/00048) and by the Department of Economic Development and Competitiveness of the  
51  
52 Basque Government (ETORTEK IE13-374 Programme). We thank Dr. Javier Calvo for mass  
53  
54 spectrometry support.  
55  
56  
57  
58  
59  
60

## REFERENCES

- (1) Hartwell, L. H.; Hopfield, J. J.; Leibler, S.; Murray, A. W. From Molecular to Modular Cell Biology. *Nature* **1999**, *402*, C47–C52.
- (2) Hecht, M.; Climent, E.; Biyikal, M.; Sancenón, F.; Martínez-Máñez, R.; Rurack, K. Gated Hybrid Delivery Systems: En Route to Sensory Materials with Inherent Signal Amplification. *Coord. Chem. Rev.* **2013**, *257*, 2589–2606.
- (3) Howes, P. D.; Chandrawati, R.; Stevens, M. M. Colloidal Nanoparticles as Advanced Biological Sensors. *Science* **2014**, *346*, 1247390–1247390.
- (4) Kowalczyk, B.; Walker, D. A.; Soh, S.; Grzybowski, B. A. Nanoparticle Supracrystals and Layered Supracrystals as Chemical Amplifiers. *Angew. Chem. Int. Ed.* **2010**, *49*, 5737–5741.
- (5) Coakley, K. M.; McGehee, M. D. Conjugated Polymer Photovoltaic Cells. *Chem. Mater.* **2004**, *16*, 4533–4542.
- (6) Shen, X.; Li, L.; Wu, H.; Yao, S. Q.; Xu, Q.-H. Photosensitizer-Doped Conjugated Polymer Nanoparticles for Simultaneous Two-Photon Imaging and Two-Photon Photodynamic Therapy in Living Cells. *Nanoscale* **2011**, *3*, 5140–5146.
- (7) Zhang, K.; Kopetzki, D.; Seeberger, P. H.; Antonietti, M.; Vilela, F. Surface Area Control and Photocatalytic Activity of Conjugated Microporous Poly(benzothiadiazole) Networks. *Angew. Chem. Int. Ed.* **2013**, *52*, 1432–1436.

1  
2  
3 (8) Manceau, M.; Bundgaard, E.; Carlé, J. E.; Hagemann, O.; Helgesen, M.; Søndergaard,  
4 R.; Jørgensen, M.; Krebs, F. C. Photochemical Stability of  $\Pi$ -Conjugated Polymers for Polymer  
5 Solar Cells: A Rule of Thumb. *J. Mater. Chem.* **2011**, *21*, 4132–4141.  
6  
7

8  
9  
10  
11 (9) Kalsin, A. M.; Fialkowski, M.; Paszewski, M.; Smoukov, S. K.; Bishop, K. J. M.;  
12 Grzybowski, B. A. Electrostatic Self-Assembly of Binary Nanoparticle Crystals with a Diamond-  
13 Like Lattice. *Science* **2006**, *312*, 420–424.  
14  
15

16  
17  
18  
19 (10) Jana, N. R.; Peng, X. Single-Phase and Gram-Scale Routes toward Nearly Monodisperse  
20 Au and Other Noble Metal Nanocrystals. *J. Am. Chem. Soc.* **2003**, *125*, 14280–14281.  
21  
22

23  
24  
25 (11) Zhang, K.; Tieke, B.; Forgie, J. C.; Skabara, P. J. Electrochemical Polymerisation of N-  
26 Arylated and N-Alkylated EDOT-Substituted Pyrrolo[3,4-C]pyrrole-1,4-Dione (DPP)  
27 Derivatives: Influence of Substitution Pattern on Optical and Electronic Properties. *Macromol.*  
28 *Rapid Commun.* **2009**, *30*, 1834–1840.  
29  
30  
31

32  
33  
34  
35 (12) Sonar, P.; Williams, E. L.; Singh, S. P.; Manzhos, S.; Dodabalapur, A. A  
36 Benzothiadiazole End Capped Donor–acceptor Based Small Molecule for Organic Electronics.  
37 *Phys. Chem. Chem. Phys.* **2013**, *15*, 7064–17069.  
38  
39

40  
41  
42  
43 (13) Hao, Z.; Iqbal, A. Some Aspects of Organic Pigments. *Chem. Soc. Rev.* **1997**, *26*, 203–  
44 213.  
45  
46

47  
48  
49 (14) Manceau, M.; Rivaton, A.; Gardette, J.-L.; Guillerez, S.; Lemaître, N. The Mechanism of  
50 Photo- and Thermooxidation of poly(3-Hexylthiophene) (P3HT) Reconsidered. *Polym. Degrad.*  
51 *Stab.* **2009**, *94*, 898–907.  
52  
53  
54  
55  
56  
57  
58  
59  
60

1  
2  
3 (15) Gierschner, J.; Cornil, J.; Egelhaaf, H.-J. Optical Bandgaps of  $\Pi$ -Conjugated Organic  
4 Materials at the Polymer Limit: Experiment and Theory. *Adv. Mater.* **2007**, *19*, 173–191.  
5  
6

7  
8 (16) Aoyama, Y.; Yamanari, T.; Ohashi, N.; Shibata, Y.; Suzuki, Y.; Mizukado, J.; Suda, H.;  
9 Yoshida, Y. Direct Effect of Partially Photooxidized poly(3-Hexylthiophene) on the Device  
10 Characteristics of a Bulk Heterojunction Solar Cell. *Sol. Energ. Mat. Sol.* **2014**, *120*, 584–590.  
11  
12  
13

14 (17) Kim, C.; Liu, J.; Lin, J.; Tamayo, A. B.; Walker, B.; Wu, G.; Nguyen, T.-Q. Influence of  
15 Structural Variation on the Solid-State Properties of Diketopyrrolopyrrole-Based  
16 Oligophenylenethiophenes: Single-Crystal Structures, Thermal Properties, Optical Bandgaps,  
17 Energy Levels, Film Morphology, and Hole Mobility. *Chem. Mater.* **2012**, *24*, 1699–1709.  
18  
19  
20  
21  
22  
23

24 (18) Scarabelli, L.; Grzelczak, M.; Liz-Marzán, L. M. Tuning Gold Nanorod Synthesis  
25 Through Pre-Reduction with Salicylic Acid. *Chem. Mater.* **2013**, *25*, 4232–4238.  
26  
27  
28  
29  
30  
31

## 32 TOC GRAPHICS

33  
34  
35  
36

